Electronic Supplementary Material (ESI) for Journal of Materials Chemistry C.

Supporting Information

Electrical Transport Characteristics of Chemically Robust PDPP-DTT Embedded in a Bridged Silsesquioxane Network

Jihye Shin[†,a,b]*, Han Wool Park*[†,c]*, Seunghan Kim*[†,a]*, Jeehye Yang*[a]*, Jaehee Kim*[c]*, Hye Won Park*[a]*,*
Do Hwan Kim[*,c] *and Moon Sung Kang*[*,a]

[a] *Department of Chemical and Biomolecular Engineering, Sogang University, Seoul 04107, Republic of Korea*

[b] *Department of Chemical Engineering, Soongsil University, Seoul 06978, Republic of Korea*

[c] *Department of Chemical Engineering, Hanyang University, Seoul 04763, Republic of Korea.*

† contributed equally to this work

*corresponding authors: kangms@sogang.ac.kr, dhkim76@hanyang.ac.kr

KEYWORDS : PDPP-DTT, semi-interpenetrating diphasic polymer network, chemical robustness, electrical transport, thin-film transistor

To form *s*-IDPN containing PDPP-DTT, PDPP-DTT and 1,8-bis(trichlorosilyl)octane were dissolved in chlorobenzene, and then the mixture solution was stirred for 1 h. The weight fraction of 1,8-bis(trichlorosilyl)octane, the organosilyl precursor, was varied. A typical mixture solution contained 9 wt% of precursors; the resulting chemically robust film prepared from this mixture solution is referred to as *cr*-PDPP-DTT (9) within this article. During the stirring, the presence of a marginal amount of moisture in chlorobenzene substituted the chlorine groups of the precursor into hydroxyl groups (Figure S1a). Subsequently, the mixture solution was spin-casted onto a substrate to form a solid thin film. Thermal annealing of the film then led to a condensation reaction between the hydroxyl groups of the neighboring precursors. [S1] In addition, time-of-flight secondary ion mass spectroscopy (ToF-SIMS) analysis carried out upon etching the film reveals that the BSSQ structure is distributed over the depth of the film without apparent macroscopic phase separation (Figure S3 and S4). Overall, we speculate that the ladder-like BSSQ framework permitting the chains of PDPP-DTT to interpenetrate into the BSSQs forms the *cr*-PDPP-DTT film in the s-IDPN structure.

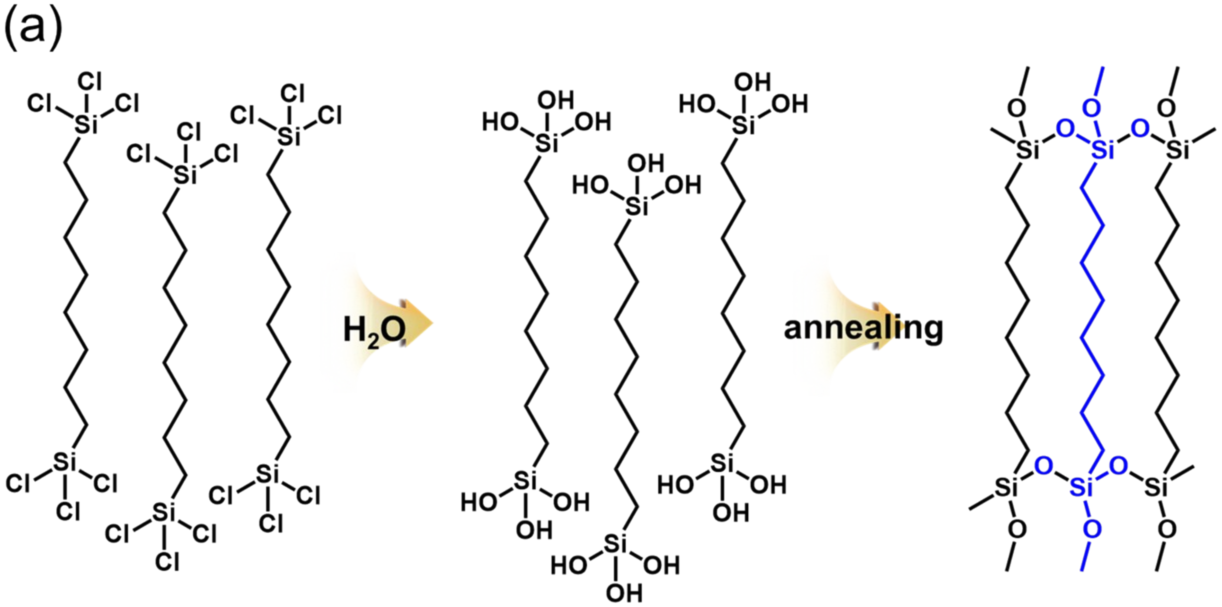

Figure S1. (a) Schematic representation showing the hydrolysis of the precursor molecules and the following condensation reaction forming the BSSQ network.

The *cr*-PDPP-DTT exhibited chemical robustness against organic solvents. This was confirmed first by comparing the thickness and morphology of the films that were partially dipped into organic solvents used for processing PDPP-DTT for 1 min. The solvents were chloroform, chlorobenzene, and hot chlorobenzene (80°C); chlorobenzene was, in fact, the mother solvent for the polymer semiconductor-organosilyl sol in the experiment. The AFM images (Figure S2a) also confirm that the dipping process does not produce a noticeable change in the plane-view morphology of the *cr*-PDPP-DTT (9) film. We emphasize that a slight increase in surface roughness was noticed; the roughness *R*q of 0.985 nm (obtained from a 5-µm × 5-µm image) obtained from an undipped *cr*-PDPP-DTT (9) film increased to 1.28 nm, and it became 1.56 nm after the film was dipped into chloroform and hot chlorobenzene, respectively. Despite the small change in the film roughness, the results overall indicate that *cr*-PDPP-DTT exhibits good chemical robustness against solvents that can effectively dissolve pristine PDPP-DTT. As a reference, we carried out the same experiment on a pristine PDPP-DTT film (thickness = 50 ± 4 nm). Because the pristine film was entirely removed after briefly dipping it into the solvents, the thickness measurement as well as the morphology measurement could not be carried out.

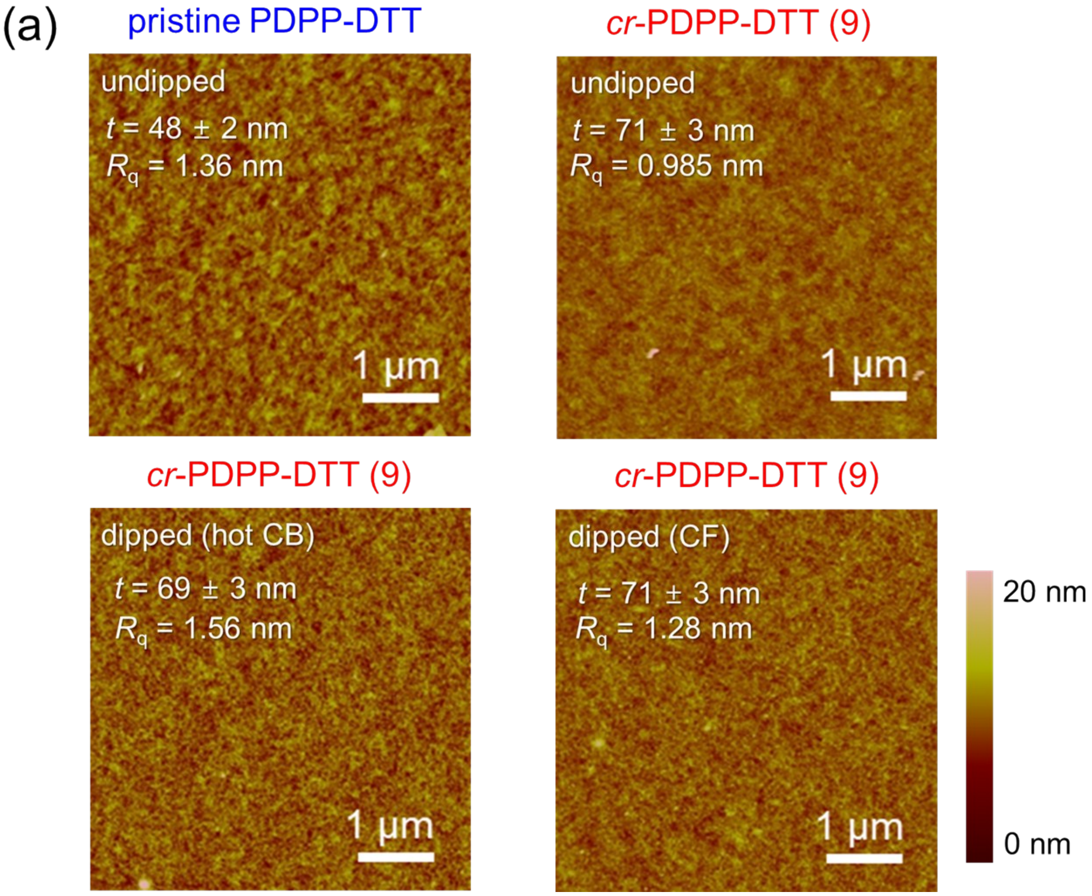

Figure S2. (a) AFM images of the pristine PDPP-DTT film (undipped region) and the *cr*-PDPP-DTT (9) film (undipped and dipped regions) that were partially treated with hot chlorobenzene/chloroform.

Time-of-flight secondary ion mass spectroscopy (ToF-SIMS) analysis was carried out upon etching the PDPP-DTT films. Figure S3a and b show the signal distribution of the elements (S^- and Si^-) obtained from a pristine PDPP-DTT film and a *cr*-PDPP-DTT (19) film, respectively. The signal for S^- reflects the spatial distribution of PDPP-DTT over the film thickness. Meanwhile, the signal for Si^- reflects the spatial distribution of BSSQ structure over the film thickness. Also, the contribution originating from the Si/SiO_2 substrate would also be included in the Si^- signal. In fact, from the position of the data where the plateau in the Si^- signal appears, one can estimate the thickness of the polymer film (50 nm for the pristine PDPP-DTT film and 55 nm for the *cr*-PDPP-DTT (19), which match well with the values obtained from separate thickness measurement experiment). We note that the sharp increase in the Si^- signal that appears just before it levels off does not necessarily mean that more Si^- sources are present in the very bottom layer of the polymer film. Instead, this range of film thickness can be considered as the regime influenced by the signal coming from the substrate. Although a quantitative conclusion can be hardly drawn from the data, the comparison between Figure S3 and S4 reveals that the BPSQ framework is distributed uniformly over the *cr*-PDPP-DTT (19) film, without apparent macroscopic phase separation.

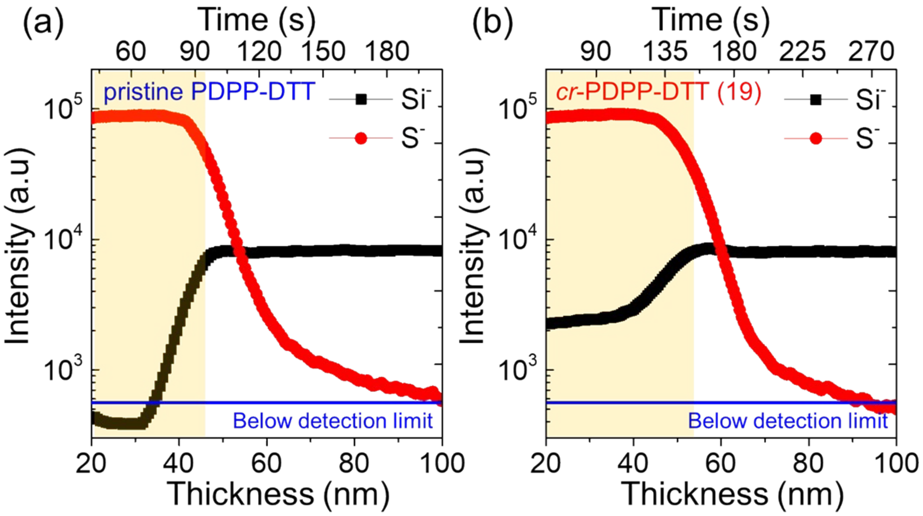

Figure S3. ToF-SIMS profiles of (a) a pristine PDPP-DTT film and (b) a *cr*-PDPP-DTT (19) film.

pristine PDPP-DTT

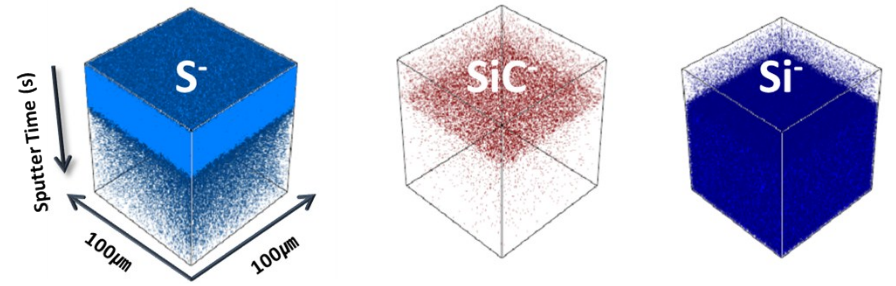

cr-PDPP-DTT (19)

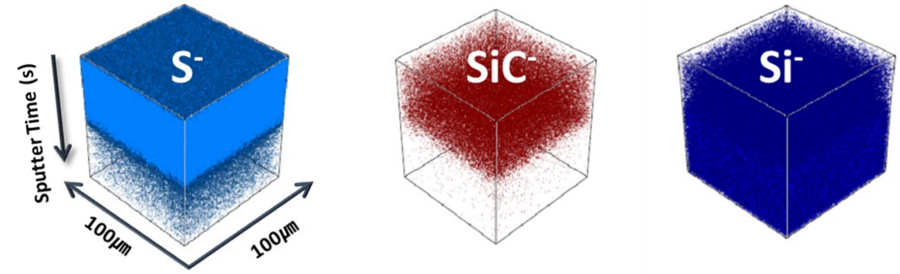

Figure S4. ToF-SIMS 3D mapping of a pristine PDPP-DTT film and a cr-PDPP-DTT (19) film for S^-, SiC^- and Si^-.

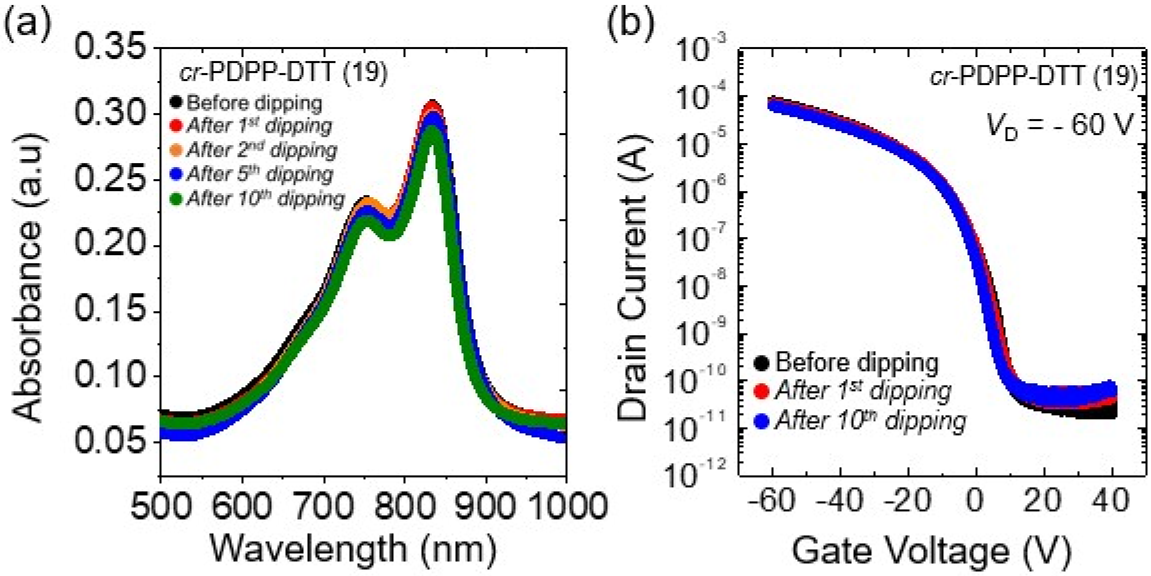

Figure S5. (a) A series of UV-Vis spectra of *cr*-PDPP-DTT (19) obtained after 0, 1, 5, and 10 cycles of dipping in chloroform. (b) A series of transfer characteristics of a transistor based on the *cr*-PDPP-DTT (19) film collected after 0, 1 and 10 rounds of dipping in chloroform.

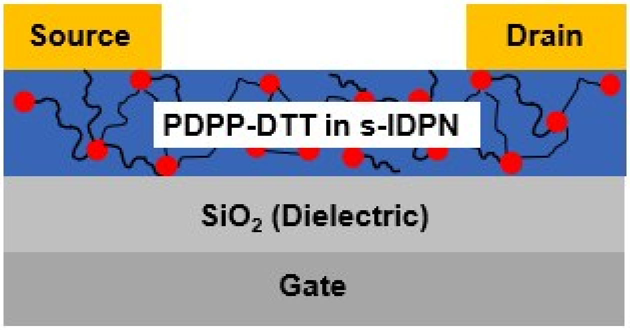

Figure S6. Schematic cross-section of a TFT based on a chemically orthogonal PDPP-DTT film

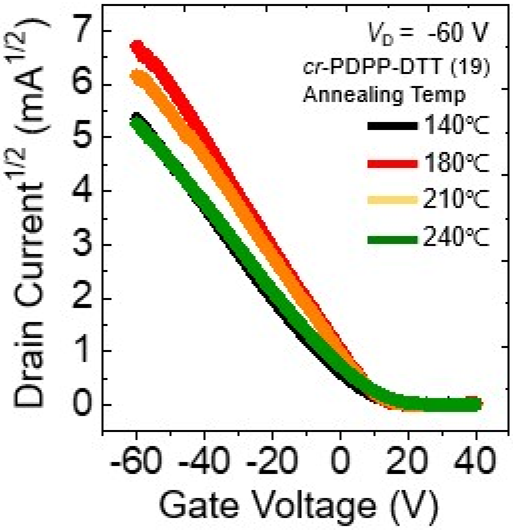

Figure S7. Transfer characteristics of the *cr*-PDPP-DTT-based TFTs prepared at different annealing temperatures (140, 180, 210, and 240 °C).

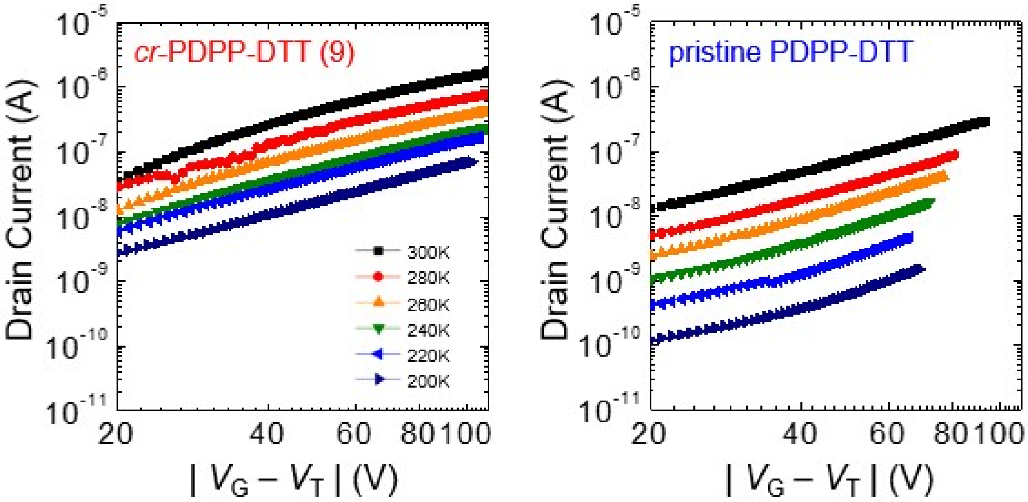

Figure S8. Double-logarithmic plots of I_D vs. $|V_G - V_T|$ at different temperatures for PDPP-DTT films.

Reference

[S1] E. S. Park, H. W. Ro, C. V. Nguyen, R. L. Jaffe and D. Y. Yoon, *Chem. Mater.,* 2008, **20**, 1548-1554.